

SCHOOL OF

•NUCLEAR
ENGINEERING

COO-2826-9

PNE-78-132

FAST BREEDER BLANKET FACILITY
Quarterly Progress Report
for the Period April 1, 1978
— June 30, 1978

Edited by
F. M. Clikeman

Prepared for
The U.S. Energy Research and
Development Administration
Under Contract No. EY-76-S-02-2826

June, 1978

Purdue University, West Lafayette, Indiana 47907

DISTRIBUTION OF THIS DOCUMENT IS UNLIMITED

DISCLAIMER

This report was prepared as an account of work sponsored by an agency of the United States Government. Neither the United States Government nor any agency Thereof, nor any of their employees, makes any warranty, express or implied, or assumes any legal liability or responsibility for the accuracy, completeness, or usefulness of any information, apparatus, product, or process disclosed, or represents that its use would not infringe privately owned rights. Reference herein to any specific commercial product, process, or service by trade name, trademark, manufacturer, or otherwise does not necessarily constitute or imply its endorsement, recommendation, or favoring by the United States Government or any agency thereof. The views and opinions of authors expressed herein do not necessarily state or reflect those of the United States Government or any agency thereof.

DISCLAIMER

Portions of this document may be illegible in electronic image products. Images are produced from the best available original document.

NOTICE

This report was prepared as an account of work sponsored by the United States Government. Neither the United States nor the United States Department of Energy, nor any of their employees, nor any of their contractors, subcontractors, or their employees, makes any warranty, express or implied, or assumes any legal liability or responsibility for the accuracy, completeness or usefulness of any information, apparatus, product or process disclosed, or represents that its use would not infringe privately owned rights.

TABLE OF CONTENTS

TASK B	
(R.C. Borg and R.H. Johnson)	1
B.1. Introduction	1
B.2. Safety Investigations	
(R.C. Borg and T.F. Lin)	2
B.2.1. Introduction	2
B.2.2. Results and Discussions	3
B.2.3. Conclusions	7
B.3. Cross Section Preparation	
(R.C. Borg, R.H. Johnson and M.P. Sohn)	8
B.4. Neutron Spectral Comparisons	
(J.H. Paczolt, M.P. Sohn, R.H. Johnson and R.C. Borg)	9
 TASK C	
(F.M. Clikeman)	14
C.1. Testing Experimental Equipment and Techniques	
(F.M. Clikeman, R.H. Johnson, D.W. Vehar, G.A. Harms H.P. Chou and K.R. Koch)	14
C.1.1. Foil Activation Measurements	
(G.A. Harms and F.M. Clikeman)	14
C.1.2. Proton-Recoil Proportional Counting	
(D.W. Vehar and F.M. Clikeman)	16
C.1.3. Fission Rate Measurements	
(H.P. Chou, R.H. Johnson and F.M. Clikeman)	18
C.1.4. Gamma-Ray Dosimetry Measurements Using TLD Dosimeters	
(K.R. Koch and F.M. Clikeman)	21
C.2. Installation and Testing of Facility Equipment and Preparation of Operating Procedures	
(R.H. Johnson and F.M. Clikeman)	22
C.2.1. Measurement of the k_{eff} of the Fast Breeder Blanket Facility	
(F.M. Clikeman)	23
C.2.2. Californium-252 Source Neutron Emission Rates	
(R.H. Johnson)	24
C.2.3. Comparison of Shielding Measurements and Calculations for the FBBF	
(R.H. Johnson)	24
C.3. Experimental Measurements Using the FBBF Facility	
(G.A. Harms and F.M. Clikeman)	29

fey

LIST OF FIGURES

Figure C.1:	Block diagram of the automatic scanning system.	19
Figure C.2:	An enlarged positive print of fission fragment tracks registered in a microscope slide; the area of the frame has been scanned.	20
Figure C.3:	The scanned picture of the frame area in Fig. C.3. . . .	30
Figure C.4:	Radial and azimuthal positions.	33
Figure C.5:	Radial traverse of gold saturated activities both bare and cadmium covered.	34
Figure C.6:	Axial traverse of bare gold activity at position A-1. . .	35
Figure C.7:	Axial traverse of bare gold activity at position A-6. . .	36
Figure C.8:	Axial traverse of bare gold activity at position A-12. .	37
Figure C.9:	Axial traverse of bare gold activity at position A-17. .	38
Figure C.10:	Axial traverse of gold activity both bare and cadmium covered.	39
Figure C.11:	Azimuthal traverse of bare gold activity at radius 32.5 cm.	40
Figure C.12:	Azimuthal traverse of bare gold activity at radius 32.5 cm. (zero suppressed).	41
Figure C.13:	Reproducibility test of the FBBF using manganese foils. .	42
Figure C.14:	Radial traverse of saturated manganese activity.	43

LIST OF TABLES

Table B.1:	Effective Multiplication Factors for Various Dry-Flooded Conditions for SS Double Clad Blanket with a Pitch of 0.673 Inch	10
Table B.2:	Effective Multiplication Factors for Various Dry-Flooded Conditions for SS Double Clad Blanket with a Pitch of 0.900 Inch	11
Table B.3:	Effective Multiplication Factors for Various Dry-Flooded Conditions for Al Double Clad Blanket with a Pitch of 0.900 Inch	11
Table B.4:	K-infinity for Inner Converter Outer Converter and Blanket Under Various Conditions	12
Table B.5:	Effective Multiplication Factors Calculated by Various Models for 0.673 inch SS Double Clad Blanket Under Various Conditions Without Boron in Converters	13
Table C.1:	Size and Location of Californium Sources	25
Table C.2:	Dose Rates	28
Table C.3:	Radial and Azimuthal Positions	44

ABSTRACT

The work performed in the reporting period was primarily concerned with the initial measurements and checkout of the Purdue Fast Breeder Blanket Facility (TASK C). The safety calculations for the "as built" are also presented and compared with the initial safety calculations (TASK B).

Safety calculations on the FBBF facility have been completed for a variety of new flooded-dry combinations. Specifically the effect of adding boron carbide to the transformer regions was investigated. The investigation showed the stabilizing effect of the boron carbide in the flooded cases while the effect in the dry cases is minimal (B.2).

Measurements of the k_{eff} of the FBBF facility, of the effectiveness of the shielding, and of the radiation levels in the rooms surrounding the laboratory have been completed and compare well with the calculations presented in the license application (C.2).

Progress continues to be made in the development of measurement techniques for use with the FBBF facility (C.1). Work is also progressing on the preparation of a new cross section set that will better represent the conditions in the FBBF (B.3) and will permit more accurate spectra calculations (B.4). Initial gold and manganese foil activation measurements in the radial direction and gold activation measurements in the axial and azimuthal directions have been completed and the initial results are presented (C.3).

TASK B
(R.C. Borg and R.H. Johnson)

B.1. Introduction

The object of this task is to perform a detailed analysis of the current FBBF loading and a detailed preanalysis of future loadings. In Sec. B.2., results are reported for the ongoing safety investigations of the current and future loadings. The inherent safety features of the FBBF have been studied with the converter (transformer) regions either dry or flooded; several different calculational techniques have been compared. Progress on the preparation of a cross section set self-shielded for room temperature is reported in Sec. B.3. Comparisons of reaction rates calculated using diffusion and discrete ordinates codes have been reported previously; progress on comparison of spectra calculated using different codes is reported in Sec. B.4.

Two papers on the FBBF have been presented.^{1,2} These papers described the facility, the preanalysis calculations, and the experimental measurements.

B.2. Safety Investigations
(R.C. Borg and T.F. Lin)

B.2.1. Introduction

In the previously reported safety investigations of the hypothetical accident, all regions of the FBBF were assumed to be flooded. The effects of boron with dry rather than flooded converters were not considered in these earlier studies. Initially one-dimensional FOG code calculations were used to evaluate k_{eff} for various dry-flooded conditions for the presumed initial loading configuration without boron in the converters.³ Later, two models for the mockup of the FBBF, one with and one without explicit treatment of B_4C transition regions, were used with the two-dimensional 2DB code.⁴ The value of k_{eff} for specified conditions such as pitch variation and the type of secondary cladding for hypothetical accident conditions were evaluated. These investigations indicated that, for a number of blanket pitches with Al as secondary clad, the value of k_{eff} could be about 0.8. In order to re-evaluate these few cases, the converters were considered dry rather than flooded.

The object of this study is to investigate the inherent safety feature of the FBBF with both the inner and outer converters dry or flooded and also to verify the initial calculations with the improved methods. Because the converters are both separately constructed and sealed by welding, it is feasible and necessary to evaluate the flooding of the FBBF with dry converters.

The composition of each region of the FBBF in this study was determined from the initial loading configuration. The radial blanket, which physically has inner rows of SS double clad natural uranium fuel pins and outer rows of Al double clad pins, was modified for the calculations by considering an all Al or SS double clad blanket. Also two blanket pitches were chosen for

investigation of the effect of pitch variation under various dry-flooded conditions. The initial blanket loading pitch, 0.673 inch and the pitch of the maximum reactive configuration, 0.900 inch, i.e., the configuration which results in maximum k_{eff} , were used.⁴

The pitch in the inner converter is slightly increased from the original design value of 0.468 inch to 0.474 inch. The amounts of natural B_4C vibrated into the inner and outer converters are 21.59 kg and 23.313 kg, respectively. It occupies 61.24 percent of the possible voided volume of the inner converter and 53.58 percent of the outer converter. These amounts of B_4C are very close to the previously assumed value of 60 percent.⁴ The source region was considered to be flooded with and without the source plug in order to compare results with the previous investigations.³ Because the reflectors are also welded shut, they were treated as dry regions for most of the cases investigated.

The unit cell set up for the input to the HAMMER code⁵ for generating group constants in each region is the same as that used previously.⁴ Two models were used to mock up the facility, one included B_4C transition regions and the other did not. They are presented in Ref. 4. The corrected material number densities and explicit dimensions of the facility used here are presented in Ref. 6.

B.2.2. Results and Discussions

The effective multiplication factors, calculated with the model which explicitly treats the transition regions, for various conditions are presented in three tables. Table B.1 gives values of k_{eff} for a pitch of 0.673 inch, Table B.2 for a pitch of 0.900 inch with a SS double clad blanket and Table B.3 for a pitch of 0.900 inch with Al as secondary cladding. The k -infinite values which are helpful in understanding the results are given

in Table B.4 for the converters and blankets.

Several important features of the FBBF are found in this investigation. They are discussed in the following.

(1) Boron effect:

The presence of B_4C in the converters stabilizes the value of k_{eff} for a given blanket pitch irrespective of whether the converters are dry or flooded (compare the first four cases in Tables B.1, B.2 and B.3). Every region in the FBBF has some contribution to the value of k_{eff} , but the degree of its influence depends on the magnitude of k_∞ , and the size and the location of the region. All of the fuel of the FBBF is loaded in the converters and blanket, therefore, these regions have the dominate impact on the determination of the value of k_{eff} . The values of k_∞ as shown in Table B.4, for flooded converters with boron are only slightly smaller than the k_∞ values of the dry converters with boron (comp. Cases No. 2, 4, 6 and 8 in Table B.4). This trend is due to the compensation between the increased absorption of B_4C and fission of U-235 as the neutron spectrum becomes softer for the flooded case. Therefore, if boron is in the converters, there is not much difference in the k_{eff} results since the k_∞ value of the converters do not significantly change when comparing the dry and flooded cases.

For the boron free cases, k_{eff} greatly increases if the dry converters are assumed to be flooded for the same blanket (compare the last four cases in Tables B.1 and B.2). This increase is more pronounced for the initial loading pitch. The values of k_∞ are much smaller for the dry converters without boron than the flooded converters without boron (compare cases No.1, 3, 5 and 7 of Table B.4). All of these values of k_∞ are sufficiently larger than k_∞ of the blanket with the initial loading pitch. For the blanket

with a pitch of 0.900 inch the value of k_{∞} is larger than case 5 and substantially larger than case 9 (compare cases No. 1, 3, 5, 7, 9 and 10 of Table B.4). Therefore, the converters have a larger influence on the values of k_{eff} for the case of the blanket with the initial loading pitch, while the blanket has proportionately a greater contribution for the case with a pitch of 0.900 inch. Thus, one would expect k_{eff} to increase when comparing cases with dry and flooded converters. Also, the increases should be more pronounced for the case with the blanket initial loading pitch as is indicated in Tables B.1 and B.2. Case 9 in Table B.2 considered all regions of the FBBF flooded; as illustrated in the table, the value of k_{eff} is identical to that of case 8 which has a dry reflector. Thus, the impact of a dry versus wet reflectors is minimal.

(2) The effect of water in source region:

For the cases with boron in the converters, k_{eff} changes very little even if the stainless steel plug in the source region is replaced with water for both SS and Al double clad blankets (compare the first four cases in Tables B.1, B.2 and B.3).

The water in source region can soften the neutron spectrum in the adjacent regions, and thus influence these regions. The boron in the converters has a stabilizing effect as stated above. Which one of these effects is more important depends on the values of k_{∞} in the converters and the blanket. Since the values of k_{∞} for the converters with boron are not much larger than those of blankets (compare cases No. 2, 4, 6, 8, 9, 10 and 11 of Table B.4), the boron stabilizing effect is dominant. Therefore, the replacement of the SS source region with water has negligible effect on the values of k_{eff} for the cases with boron in the converters.

For the boron free converters, k_{eff} has a negligible change in the dry cases, but has a slight increase in the flooded cases when the stainless steel plug

in the source region is replaced with water (compare the last four cases in Tables B.1 and B.2). Since no boron stabilizing effect exists, the values of k_{eff} are influenced by the effect of water in the source region which in turn depends on the k_{∞} of the converters and the blanket. The values of k_{∞} for the flooded converters without boron are much larger than those of SS double clad blankets (compare cases No. 3, 7, 9 and 10 of Table B.4). Therefore, in water the source region has a larger influence for the flooded cases without boron.

(3) The effect of pitch variation:

The value of k_{eff} increases as the pitch of the blanket increases from 0.673 inch to 0.900 inch. This is consistent with the previous investigations.⁴ This is due mainly to the increase in k_{∞} from 0.4705 for the pitch 0.673 inch to 0.6831 for the pitch 0.900 inch SS double clad blanket (compare cases No. 9 and 10 of Table B.4).

(4) SS double clad vs Al double clad:

If the Al double clad fuel pins are used instead of SS double clad fuel pins, k_{eff} increases. This is consistent with the previous investigations. Comparing the last two cases in Table B.4, k_{∞} increases from 0.6831 to 0.8583 for this change in the blanket.

(5) The comparison of models:

The values of k_{eff} calculated by the three models described in the introduction are given in Table B.5 for the boron-free cases with the blanket pitch of 0.673 inch. Models 1 and 2 are used with the two-dimensional 2DB calculation with and without the transition regions treated, respectively. Model 3 is the basis of the one-dimensional FOG calculation.³

The values of k_{eff} obtained from Models 2 and 3 agree very well, but are a little higher than those evaluated from Model 1 for the dry cases.

while the converse is true for the flooded case. The increasing trend in k_{eff} from the dry case to flooded case is the same for the three models.

The improved two-dimensional model, Model 3, which is the basis of present investigation, should give more reliable results. The results of Model 3 are consistent with those from Model 2, however.

B.2.3. Conclusions

The use of improved methods and models in the present safety investigation of a hypothetical flooding accident has led to several important conclusions which are summarized here.

- (1) Boron in the converters has a stabilizing effect irrespective of whether they are treated as dry or flooded cases, i.e., for a hypothetical accident k_{eff} stays fairly constant when B_4C is present in the converters. If there is no B_4C in the converters, k_{eff} would greatly increase from the dry case to flooded case. However, boron in the converters still can not bring the values of k_{eff} below 0.75 for Al double clad blanket with the pitch of 0.900 inch (Table B.3).
- (2) The replacement of the stainless steel in the source region with water has only negligible effect on the FBBF except for the case of the flooded converters without boron.
- (3) Flooded reflectors have little impact on the value of k_{eff} .
- (4) The pitch variation from the initial loading pitch to maximum reactive pitch of SS double clad blanket results in an increase in k_{eff} (Ref. 4).
- (5) The change from SS double clad blanket to Al double clad blanket also results in an increase in k_{eff} (Ref. 4).
- (6) The results from the three models are in fairly good agreement and the trends for different dry-flooded conditions are the same.

B.3. Cross Section Preparation

(R.C. Borg, R.H. Johnson and M.P. Sohn)

The computer code ⁷IDX, a one-dimensional diffusion code for generating resonance self-shielded and collapsed group cross sections, has recently been modified and tested. A fixed source option which was added was tested against a reference case calculated with ⁸2DB, and was found to be working properly.

Work is currently underway to collapse a new group constant set from the 50-group, 101-isotope DLC-40 LIB-IV, library.⁹ These new group constants will be used for improved reaction rate calculations for the current FBBF loading.

B.4. Neutron Spectral Comparisons

(J.H. Paczolt, M.P. Sohn, R.H. Johnson and R.C. Borg)

As part of the preanalysis, gamma-ray heating rate calculations were performed using a modified 23N-21G* coupled cross section set¹⁰ and the discrete ordinates code ANISN-W.¹¹ A comparison of the neutron spectra generated with the transport and diffusion codes at various radial positions along the active midplane is underway. The spectra were calculated using ANISN-W, LAZARUS¹² (a one-dimensional diffusion code) and 2DB⁸ (a two-dimensional diffusion code). The purpose of this comparison is to verify that the results of the transport and diffusion calculations performed in the preanalysis are consistent.

* Read as 23 neutron groups, 21 gamma-ray groups.

TABLE B.1

Effective Multiplication Factors
 for Various Dry-Flooded
 Conditions for SS Double Clad Blanket
 with a Pitch of 0.673 Inch

Case No.	Source	IC	OC	B_4C	Blanket	Reflector	k_{eff}
1	SS	D	D	Y	F	D	0.41027
2	SS	F	F	Y	F	D	0.40507
3	F	D	D	Y	F	D	0.41259
4	F	F	F	Y	F	D	0.40693
5	SS	D	D	N	F	D	0.46846
6	SS	F	F	N	F	D	0.72101
7	F	D	D	N	F	D	0.46953
8	F	F	F	N	F	D	0.76546

The symbols used in the table:

IC - Inner converter

OC - Outer converter

SS - Stainless Steel plug

D - Dry

F - Flooded

Y - B_4C in converters

N - No B_4C in converters

TABLE B.2

Effective Multiplication Factors
for Various Dry-Flooded
Conditions for SS Double Clad Blanket
with a Pitch of 0.900 Inch

Case No.	Source	IC	OC	$B_4 C$	Blanket	Reflector	k_{eff}
1	SS	D	D	Y	F	D	0.61864
2	SS	F	F	Y	F	D	0.61668
3	F	D	D	Y	F	D	0.61858
4	F	F	F	Y	F	D	0.61669
5	SS	D	D	N	F	D	0.64959
6	SS	F	F	N	F	D	0.75855
7	F	D	D	N	F	D	0.64974
8	F	F	F	N	F	D	0.79170
9	F	F	F	N	F	F	0.79171

The symbols used here are the same as Table B.1.

TABLE B.3

Effective Multiplication Factors
for Various Dry-Flooded
Conditions for Al Double Clad Blanket
with a Pitch of 0.900 Inch

Case No.	Source	IC	OC	$B_4 C$	Blanket	Reflector	k_{eff}
1	SS	D	D	Y	F	D	0.77529
2	SS	F	F	Y	F	D	0.77168
3	F	D	D	Y	F	D	0.77518
4	F	F	F	Y	F	D	0.77167

The symbols used here are the same as Table B.1.

TABLE B.4

K-infinity for Inner Converter
Outer Converter and
Blanket Under various Conditions

Case	Region	Conditions	K_∞
1	IC	dry, no B_4C	0.7905
2	IC	dry, with B_4C	0.5589
3	IC	flooded, no B_4C	0.9403
4	IC	flooded, with B_4C	0.5218
5	OC	dry, no B_4C	0.6576
6	OC	dry, with B_4C	0.4539
7	OC	flooded, no B_4C	0.7755
8	OC	flooded, with B_4C	0.4493
9	Blanket	flooded, 0.673 inch SS double clad	0.4705
10	Blanket	flooded, 0.900 inch SS double clad	0.6831
11	Blanket	flooded, 0.900 inch Al double clad	0.8583

IC - Inner Converter

OC - Outer Converter

TABLE B.5

Effective Multiplication Factors
 Calculated by Various Models
 for 0.673 inch
 SS Double Clad Blanket Under Various Conditions
 Without Boron in Converters

Case No.	Model	Source	IC	OC	Blanket	Reflector	k_{eff}
1	1	SS	D	D	F	D	0.46846
2	1	SS	F	F	F	D	0.72101
3	1	F	D	D	F	D	0.46953
4	1	F	F	F	F	D	0.76546
5	2	SS	D	D	F	D	0.49537
6	2	SS	F	F	F	D	0.64788
7	2	F	D	D	F	D	0.56906
8	2	F	F	F	F	D	0.71030
9	3	SS	D	D	F	F	0.4884
10	3	SS	F	F	F	F	0.6486
11	3	F	F	F	F	F	0.7180

The Model No.

- 1 - model with explicit treatment of transition regions.
- 2 - model without explicit treatment on transition regions.
- 3 - one dimensional FOG calculation.

TASK C

(F.M. Clikeman)

INTRODUCTION

The objectives of this task are: 1) The testing of experimental equipment and the development of techniques for making experimental measurements in the blanket region of the FBBF facility; 2) Performing check-out tests and preparing the operating procedures required for licensing purposes and for the safe operation of the FBBF facility; 3) Performing measurements on the first blanket configuration of the FBBF. Progress of these tasks are summarized in the following section.

C.1. Testing Experimental Equipment and Techniques(F.M. Clikeman, R.H. Johnson, D.W. Vehar, G.A. Harms
H.P. Chou and K.R. Koch)

Preliminary testing of the equipment and techniques used for neutron spectroscopy, integral neutron capture rate, fission rate, and gamma dosimetry measurements continued during the quarter. The majority of the testing proceeded using the PUR-I reactor as well as radioactive sources including a small ^{252}Cf fission source. Preliminary activation measurements were made using the FBBF facility both to determine the characteristics of the facility and to test the techniques that will be used in the foil activation measurements. Results of the preliminary foil activation measurements will be reported under Sec. C.3.

C.1.1. Foil Activation Measurements

(G.A. Harms and F.M. Clikeman)

During the progress period the techniques and data reduction methods that had been developed for determining the activity of foils activated in the

FBBF facility were tested. Gold, manganese and depleted uranium foils were activated in the FBBF facility and counted using the high resolution Ge(Li) detector and Canberra data acquisition system. The preliminary measurements show that on the basis of one foil irradiation that the activities from gold could be determined with a standard deviation of 1%, that the activities of manganese could be determined with a standard deviation of 2%, and that the activities of the neptunium produced by neutron capture in U-238 could be determined to about 1% at the transformer-blanket interface. (Note: The standard deviation used here include only the standard deviations from the counting statistics and does not include the uncertainties in the determination of the efficiency of the detector system or any systematic errors.) More complete results of gold and manganese experiments are reported in Sec. C.3. The preliminary experiments also indicated that on the basis of a single irradiation, the activity of the neptunium at the blanket-reflector interface could be determined to a standard deviation of about 12%.

Most of the preliminary calculations and sensitivity studies of the FBBF have indicated that standard deviations in the measured reaction ratio of the order of 1% are required throughout most of the blanket regions if meaningful comparisons with calculated reaction rates are to be made. For the U-238 capture reaction, 2% standard deviations are required in the blanket.¹³ It is obvious from the above measurement that if a standard deviation of 1%-2% is to be achieved that repeated measurements of the activity produced at each point would have to be made and the results added together. To determine the validity of this concept of adding the results of numerous measurements together in order to reduce the standard deviation, a set of preliminary manganese foils were activated at the same position in the FBBF blanket. The results showed that by correcting for the decay of the californium source, the results of

the individual measurements are consistent within a standard error determined only by the counting statistics of each run. However, these results, using the manganese foils, have a standard deviation of 2% and it is intended to repeat the experiment using a different activity that will yield considerably higher counting rates and therefore smaller standard deviations in the counting statistics.

C.1.2. Proton-Recoil Proportional Counting (D.W. Vehar and F.M. Clikeman)

During the quarter the new versions PSNS series of data reduction codes were adapted for use with the PDP-11/04 computer. The codes were tested using several measurements taken with the proton-recoil spectrometer system and the PUR-I reactor. The new programs gave results that agreed with the results of the earlier data analysis programs.

As a means of verifying the proper operation of the proton-recoil detectors to be used for neutron energy-spectrum measurements in the FBBF, a "neutron filter tube" was constructed for use in the PUR-I reactor pool. The neutron filter tube, consisting of a 1-1/2 inch diameter PVC pipe, provides a beam of neutrons from the PUR-I. The detector is placed with its axis perpendicular to the beam. Up to 11 inches of material, 1-1/2 inches in diameter, can be placed in the tube, so that the material's effect on the neutron energy-spectrum of the beam can be determined. By comparing structure in the measured spectra with the neutron cross section curves for the various materials, information regarding the detector operation can be obtained. In particular, the validity of the energy calibration for the detector can be checked.

Several materials are currently of interest. Iron-56 has a "window" in the total cross section at about 23 keV and a resonance at about 28 keV. To

emphasize the effects of the window in the Fe cross section, 11 inches of material is used.

Flourine-19 has several resonances in the energy range of interest; at 18, 49, and 100 keV. Flourine is readily available in the form of Teflon ($(CF_2)_x$). A thickness of 6 cm of Teflon was selected in order to emphasize the effects of the resonance decreasing the overall neutron flux more than necessary.

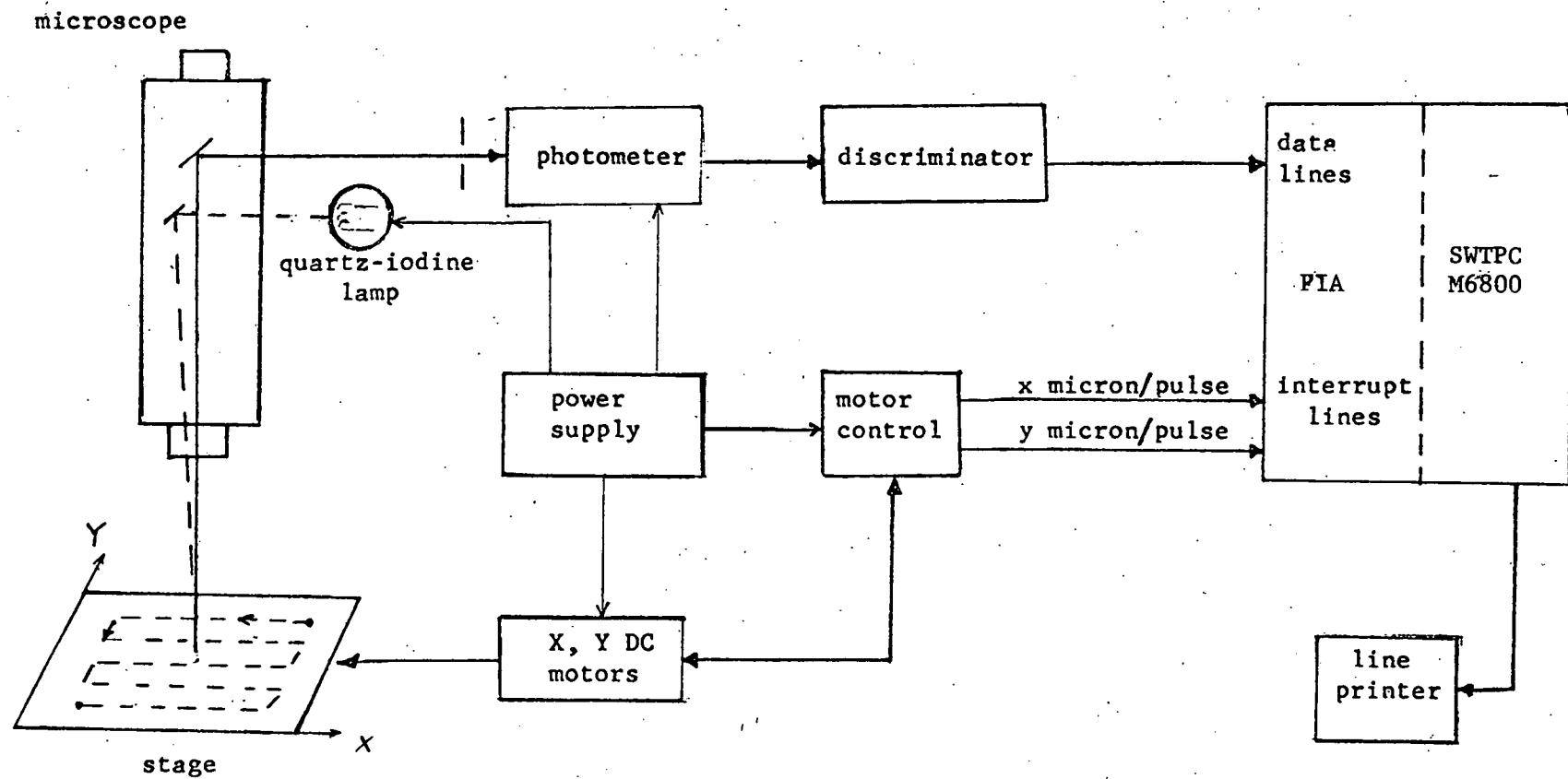
Data are obtained with a single-parameter analyser as the two-parameter analyser system is not available in the PUR-I reactor lab. Gamma-ray discrimination is performed on the basis of pulse shape; an integral discriminator is used to select a region of detector output pulse rise times which correspond to proton-recoils. It is recognized that this is not an efficient gamma-discrimination technique in the presence of high gamma-ray contribution to the total detector output, but it is satisfactory as only the location and shape of resonance effects are of interest.

Preliminary data in the 10 to 50 keV energy range have been obtained for the eight-atmosphere, H_2 proton-recoil detector. Analysis has been completed using the PSNS-N codes developed by Bennett and Yule¹⁴ without correction for electric field and wall-and-end effects. The data did not show any effect due to the Fe "window". The neutron effects may have been masked by the large gamma-ray contribution present even with pulse shape discrimination. Also, the high gamma-ray background may have worsened detector resolution due to the high count rates involved. The measurements will be repeated for both Fe and Teflon in the energy range 10 to 150 keV, using a lower reactor power to reduce the total count rate.

C.1.3. Fission Rate Measurements
(H.P. Chou, R.H. Johnson and F.M. Clikeman)

A scanning optical microscope has been interfaced with an M6800 micro-computer for the automatic counting of fission fragment tracks. The block diagram of the system is depicted in Fig. C.1. The software of the system consists of two programs. The first program is called an interrupt service routine which fetches and stores data. The second (and main) program performs track recognition and prints the results. When a hardware interrupt occurs, the main program is halted and the interrupt service routine starts to run. After the interrupt is serviced, the main program then continues the unfinished work.

Preliminary testing of the system has been made. Figure C.2 shows the picture of a portion of a microscope slide which was irradiated by a ^{252}Cf source and then, etched in 10% hydrofluoric acid for 5 minutes at room temperature. A selected area (50 x 40 microns) of the microscope slide was also scanned using the microscope. The scanned image was printed as shown in Fig. C.3. A "space" represents the track area and a "zero" represents the background area. In the scanning process, the diameter of the photometer was 3.57 microns, the X step size was 1 micron, and the Y step size was 2 microns. Comparison between Fig. C.2 and C.3 indicates that the scanned picture does represent the correct pattern; however, the track boundaries appear to be modified. The resolution of the scanned picture can be improved by using finer step size and grey level at the cost of data processing time. The process of optimizing the step size and the testing the system stability for scanning a larger area is now under way. To correct for the possible drift of the optical signal due to filament fatigue and electronic thermal drifting, an analog-to-digital converter (ADC) may be required and is being considered as a replacement for the discriminator so that the photometer threshold can be determined by software programming.



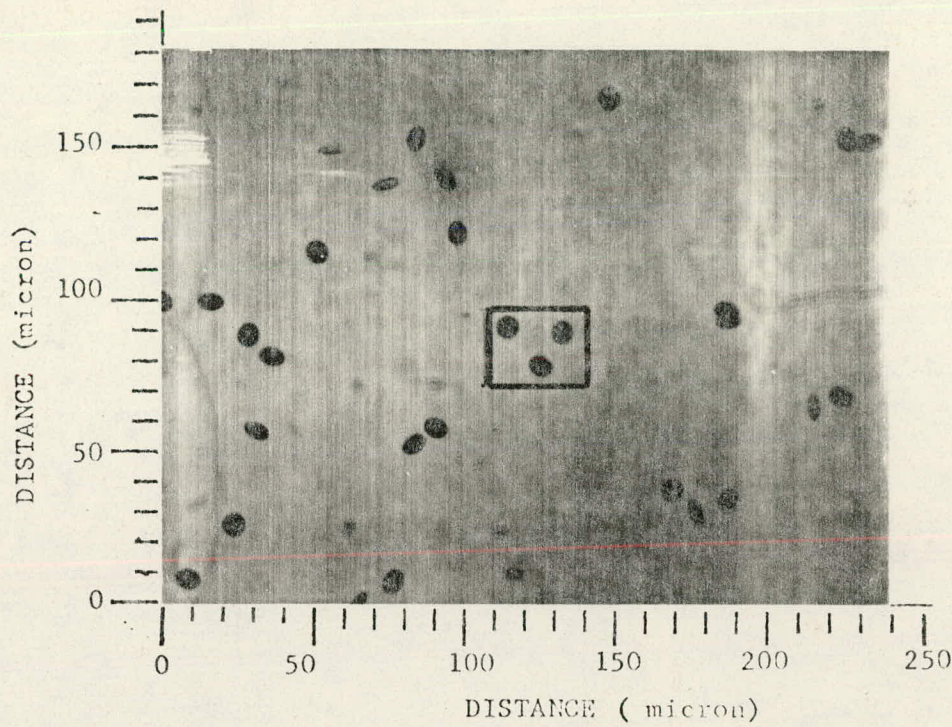


Fig. C.2: An enlarged positive print of fission fragment tracks registered in a microscope slide; the area of the frame has been scanned.

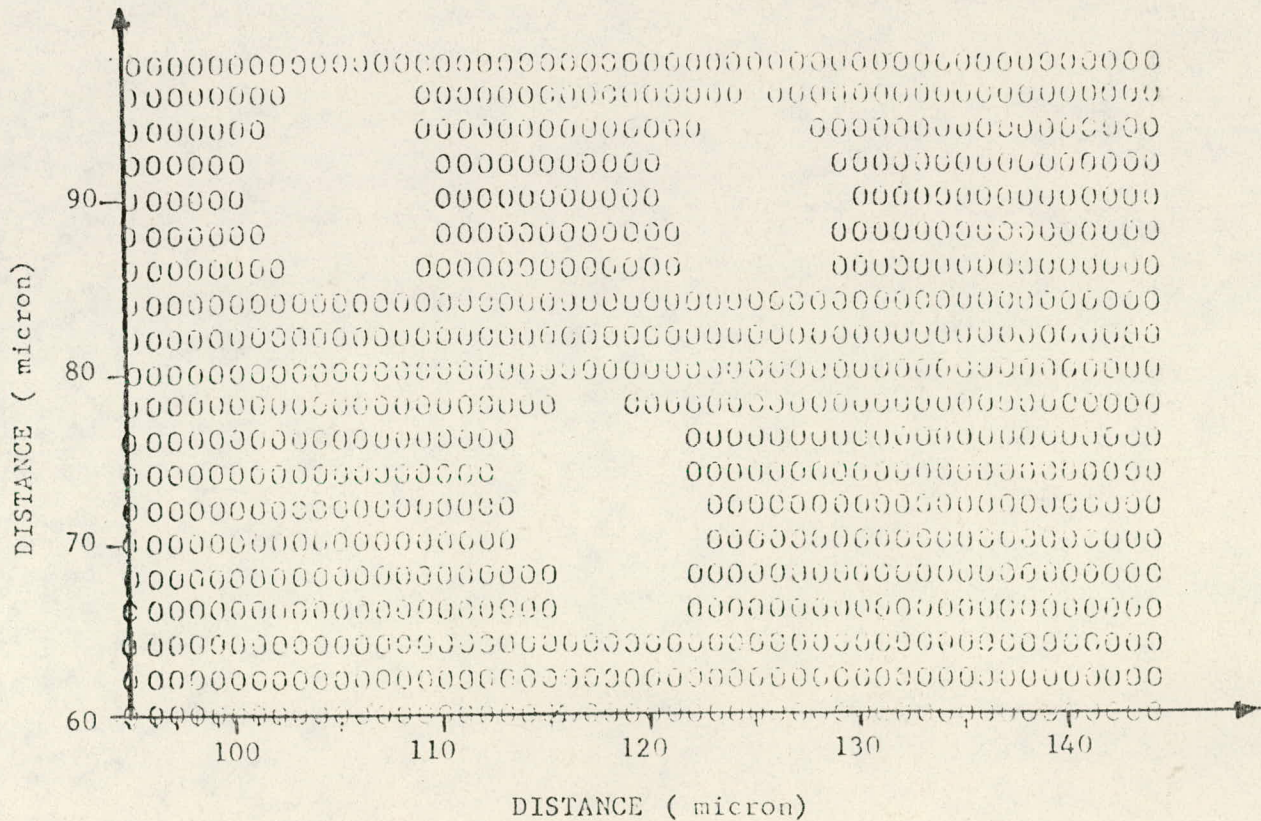


Fig. C.3: The scanned picture of the frame area in Fig. C.2.

C.1.4. Gamma-Ray Dosimetry Measurements Using TLD Dosimeters
(K.R. Koch and F.M. Clikeman)

Several irradiations of the 1/8" x 1/8" x 0.035" $\text{CaF}_2:\text{Dy}$ TLD's were made using a ^{60}Co irradiating set-up. The cobalt irradiation system utilizes a point source and a turntable capable of irradiating 60 foils at one time, insuring that each TLD receives the same exposure. The first few irradiations were used to determine glow curves so that the best TLD reader settings could be determined for the preheat temperature, the temperature ramp rate, and the integration limits. The glow curves obtained agree with the reported information having glow peaks at 130°, 180° and 220° C.¹⁶

Other irradiations were then used to determine the fading effects, the post-irradiation annealing affects on fading and accuracy, and the effects of using a nitrogen purge in the readout chamber. From all of this information the following exposure and readout procedure was determined:

1. Anneal in the metal storage trays at 400°C for 1-1/2 hr.;
2. Twenty-four hour cooling time in the metal storage trays shielded by lead;
3. Irradiation;
4. Twenty-four hour hold time; and
5. Uninterrupted readout using a 3 minute cycle
 - a) 40 sec. read
 - b) cool to 50°C and replace TLD
 - c) start new readout at $t = 3$ min.;

The TLD's are now being grouped into higher precision sets for better accuracy. The 120 TLD's used are all from the same batch. Four TLD's were eliminated due to extremely light weight. The remaining 116 TLD's had a standard deviation of 4.3%. Two sets of 58 TLD's are being formed by dividing

the range in half. The standard deviation of these sets is about 2.8%. Further accuracy will be obtained by determining correction factors for each TLD to normalized it to the set mean. From a similar sensitivity selection procedure done at Argonne,¹⁶ it appears that the standard deviation of a precision set can be reduced to about 1.7% by using correction factors.

After the correction factors for the TLD's have been determined and a final measurement of the standard deviation has been made, preliminary measurements in the FBBF will start. Both lead and stainless steel sleeves will be used to encase the TLD's in the natural uranium fuel rods in the FBBF blanket. Four TLD's placed in a symmetric pattern will be placed at each location. The average of the four readings will be used to reduce the uncertainty of the measurements. Simultaneous with the FBBF irradiations, other TLD's will be exposed to a "standard" source and these TLD's will be read out at the same time in order to permit the normalization and comparison of data taken at different times.

C.2. Installation and Testing of Facility Equipment
and Preparation of Operating Procedures
(R.H. Johnson and F.M. Clikeman)

During the month of April measurements of the k_{eff} of the FBBF facility and the radiation levels surrounding the facility and the adjacent areas in the Physics Building were completed. These measurements were required to verify the calculations used in the design of the FBBF facility. Procedures for the opening of the fuel rods to recover fuel pellets to be used in making experimental fuel rods, for operating the source drive mechanism, and for activating foils on a routine basis were developed for the FBBF facility.

C.2.1. Measurement of the k_{eff} of the Fast Breeder Blanket Facility
(F.M. Clikeman)

Subject to the conditions of the license covering the operation of the FBBF facility, measurements of the k_{eff} were completed. A PuBe neutron source together with ^3He neutron detector were used to make source multiplication measurements of the FBBF loaded with its first blanket of natural uranium rods. The neutron detector was placed in a paraffin cylinder to increase the sensitivity to epithermal and fast neutrons, giving an almost uniform sensitivity over a wide neutron energy range. Counting rates for the neutron source alone were established outside the shielded FBBF room by carefully mocking-up the source-detector spacing together with steel to represent the steel in the FBBF reflector cans. Concrete blocks were placed behind the source and detector to correct for the effects of the shielding walls of the FBBF facility. The source and detector were then positioned diagonally opposite each other in the shielded room and centered on the FBBF facility. The measured source multiplication is 1.673 ± 0.011 which yields a k_{eff} equal to 0.40 ± 0.01 . The above reported errors are due to counting statistics alone. The estimated overall error in k_{eff} is ± 0.04 . Two calculated values of k_{eff} were included in the license application. The calculated values are for the transformer regions without the boron carbide filling the interstitial regions. However, boron carbide is not expected to affect the dry (unflooded) k_{eff} . The reported calculated values were 0.400 ± 0.015 and 0.416 . Agreement between the measured and calculated values is excellent. Both the measured and calculated values are below the 0.45 value stated in the condition 15 of the SNM-142 license governing the operation of the FBBF facility.

C.2.2. Californium-252 Source Neutron Emission Rates
(R.H. Johnson)

The californium-252 source which drives the FBBF actually consists of four separately encapsulated sources (NSD-94, 95, 96 and 97) fabricated and calibrated at Oak Ridge National Laboratory (ORNL). The size and location of each of these four sources is given in Table C.1.¹⁷ The californium-252 content was given in Ref. 17 in milligrams; however, the calibration was actually a measurement of the neutron emission rate of the source by intercomparison with ORNL standard source NSS-62. A conversion factor of 2.33×10^9 n/mg was used by ORNL. Hence, the measured neutron emission rate on October 21, 1977 was $1.124 \times 10^{10} \pm 3\%$ n/s. (The error given is the standard deviation of the measured source strength on an absolute basis.)

Based on an assay of the californium used in the source fabrication, ORNL calculated the fraction of neutrons from californium-252 to be 0.99829 on the calibration date. Based on that assay, the only isotopes emitting significant numbers of neutrons are californium-250 and californium-252. An expression for the source strength of the source was found using a half-life of 2.638 ± 0.007 y for californium-252¹⁸ and 13.1 y for californium-250:¹⁹

$$S(t) = (1.124 \times 10^{10}) [9.99829 \exp(-7.194 \times 10^{-4} t) + 0.00171 \exp(-1.449 \times 10^{-4} t)] \pm 3\% \text{ n/s}$$

where t is the time in days since October 21, 1977. For the calendar year 1978, $t = (\text{day of year}) + 70$.

C.2.3. Comparison of Shielding Measurements and Calculations for the FBBF
(R.H. Johnson)

Condition 14 of the license for the FBBF states "...the licensee shall, within thirty days after start of operation of the Fast Breeder Blanket Facility

TABLE C.1

SIZE AND LOCATION
OF
CALIFORNIUM SOURCES

Source Number	^{252}Cf Content on October 21, 1977, mg	Distance of Active Center from Bottom of Source Holder, cm
NSD-96	1.015	78.0
NSD-94	1.313	57.9
NSD-95	1.307	37.6
NSD-97	<u>1.190</u>	15.2
Total	<u>4.825 \pm 3%</u>	

(FBBF), measure radiation levels outside of the facility to confirm the calculations summarized in Section E of the August 10, 1976, application, and take appropriate corrective action, if required." A short initial operation of the FBBF was carried out on April 8, 1978 with preliminary shielding measurements performed at that time. After that initial operation, planned additional shielding was added to improve the maze for the doorway to room B-28C. Later shielding measurements have been made, primarily during the period May 5-8, 1978.

The gamma-ray dose rate measurements were made using a Ludlum NaI(Tl) counter and scaler. Additional gamma-ray dose rate measurements for the preparation room, lecture room and seating area using TLD dosimeters are also being made. The neutron dose rate measurements were made using a Tracerlab "Snoopy" neutron dose rate meter. A scaler was also used with the Snoopy to improve the low level measurements.

The calculated dose rates²⁰ are based on the neutron leakage given by six-group, two-dimensional diffusion calculations;²¹ these diffusion and shielding calculations are discussed in Appendices D and E of the FBBF license application. Measured and calculated dose rates are presented in Table C.2. The neutron dose rate at the side of the FBBF (inside of the shielding) was calculated using the neutron leakage with flux-to-dose-rate conversion factors recommended by the American Nuclear Society Shielding Standards Committee. The neutron dose rate at the top of the FBBF (inside of the shielding) was calculated using fluxes from a twenty-one-group, two-dimensional diffusion calculation.

Two conclusions are drawn from the values given in the table:

1. The two-dimensional diffusion calculations appear to underpredict

the neutron leakage from the FBBF and/or to predict a too soft leakage energy spectrum.

2. The measured and calculated effectiveness of the shielding are in relatively good agreement.

Attempts to measure the dose rates in the lecture hall (room 114) and the lecture preparation room (room 114A) above the FBBF met with little success because of their small values. This was expected; the FBBF license application stated "... dose rate in rooms 114 and 114A for the source of 10^{10} neutrons/sec will probably be much too low to be measured. The shielding calculations discussed in Appendix D will therefore be used to relate the dose rates in room 114 and 114A to the dose rate on top of the FBBF shield (the ceiling of room B-28C). Measurements of dose rates near the shield can then be used to estimate the dose rates in rooms 114 and 114A."

TABLE C.2

DOSE RATES

LOCATION	CALCULATION	(mrrem/hr)		MEASUREMENT/ CALCULATION (ratio)	
		NET MEASUREMENT			
Top of FBBF (radius \approx 33 cm)	850	n ⁺	1800	n	2.1 n
Side of FBBF	74 < 1	n g	180	n	2.4 n
Top Shield Point	0.0053 n 0.018 g 0.023 total		0.0097 n 0.018 g 0.028 total	n g total	1.8 n 1.0 g 1.2 total
Side Shield Point	0.0025 n 0.0086 g 0.011 total		0.0042 n 0.0058 g 0.010 total	n g total	1.7 n 0.7 g 0.9 total
Preparation Room*	0.00061 total		0.0012 g ⁺⁺		2.0 total
Lecture Area*	0.00059 total		0.0006 g ⁺⁺		1.0 total
Seating Area*	0.000013 total		not detectable		---

*Maximum calculated and measured values for area.

⁺ Neutron dose rate indicated by n, gamma-ray dose rate indicated by g.

⁺⁺ Neutron dose rate not detectable.

C.3. Experimental Measurements Using the FBBF Facility
(G.A. Harms and F.M. Clikeman)

Foil Irradiations

The FBBF is divided into 60 degree sectors, each of which contains either 19 or 33 positions filled by removable experimental rods. Figure C.4 is a diagram of one sector showing all 33 positions and the numbering system used to designate them. The sectors are lettered A through F with Sectors A and D containing the full 33 experimental positions while the other four sectors have only the azimuthal positions. Listed in Table C.3 are the radial and azimuthal positions of the 33 experimental locations available within a sector.

Foils to be irradiated in the FBBF are placed in a thin metal cover (aluminum, cadmium, or stainless steel) and the foil-cover assembly is placed between two UO_2 pellets in an experimental rod. The experimental rod is then placed in one of the experimental positions.

Preliminary Gold Irradiations

For the first foil irradiation performed in the FBBF, 89 gold foils in aluminum covers were loaded and irradiated for 93 hours. Of these 89 foils, 17 were loaded, one per rod, near the axial midplane at the transformer regions, 46 cm above the bottom of the fuel. The remaining foils were loaded in four rods, 18 per rod and spaced about 7.5 cm apart to obtain axial distributions. The rods containing multiple foils were placed in positions 1, 6, 12, and 17 of sector A. The rods containing single foils were loaded in the remaining 13 radial experimental positions and in positions 22, 23, 33, and 34 of the same sector.

The second experiment involved the irradiation of 18 cadmium covered foils for 162 hours. Nine foils were loaded at the axial midplane in positions 1, 3, 5, 7, 9, 13, and 15 of sector A (two were in position 1), and nine foils were loaded in position A-17 spaced axially by about 15 cm.

From the foil activities measured after each irradiation, saturated activities normalized to a source strength of 10^{10} neutrons per second were calculated. All experimental results are shown with error bars at the 90% confidence level.

Figure C.5 shows results of the radial traverses for both bare and cadmium covered foils. The error bars for the data are smaller than the symbols used. The activities generated in the cadmium covered foils consistently fall only slightly below the bare foil activities indicating that the proportion of neutrons with thermal energies is small. The results also show that neutrons returning to the blanket region from the radial reflector also have energies greater than the cadmium cut off energy.

Figure C.6 through C.9 show the results of the axial traverses of bare gold foils at positions 1, 7, 12, and 17 respectively. All four figures show data that fall roughly on a cosine distribution in the region of the midplane with increases at the upper and lower boundaries of the fuel. These increases become proportionally larger as the radial position increases.

Figure C.10 shows the activity generated in the cadmium covered foils in position 17 (error bars) with the activity generated in the bare foils (circles). The cadmium covered activities fall near the bare activities at all points except the upper fuel boundary indicating that thermal neutrons contribute a very small portion of the gold activity except at the upper boundary. The thermal neutrons present at that location are considered to result from the reflection and slowing down of faster neutrons in the surrounding

concrete shielding. The increase in the activities at the lower boundary are due to reflections from the steel plate on which the whole FBBF is supported.

Azimuthal Gold Irradiation

During the assembly of the first FBBF blanket, a perturbation was introduced into the cylindrical symmetry by replacing a number of the stainless steel clad sleeves with aluminum sleeves in Sector D. An azimuthal irradiation, to check the effects of this perturbation, was made with aluminum clad gold foils located at the axial midplane and a radius of 32.5 cm from the center of the facility.

Figure C.11 shows the activities generated, plotted as a function of angular position from the center of Sector A. The center of Sector D with the extra aluminum cladding is at 180° . Figure C.12 shows the same results with the zero of the activity axis suppressed. Also shown as a solid line is the average value of all measurements. The two figures show that with the 90% confidence level at which the measurements are reported, a measurable asymmetry in the facility exists. The maximum amplitude of the effect is about 3% of the gold activity generated at the radial distance of 32.5 cm. Additional measurements and calculations of the asymmetry are now being made.

Manganese Irradiations

In order to provide a test of the two dimensional diffusion calculations of manganese reaction rates already made with the 2DB code and to check the reproducibility of measurements made in the FBBF, a series of irradiations of manganese foils at the axial midplane and various radial locations were made in Sector A. Three foils were kept in the facility under irradiation and were rotated out for counting as new foils were brought in. Four or more separate irradiations were made at positions 1, 10, 12, and 17 to check the reproducibility of the measurements.

Shown in Figure C.13 are the activities generated in the four positions as a function of time with the average values being indicated by the solid lines. The radii at which the measurements were taken are (from top to bottom) 23.7 cm, 50.3 cm, 56.3 cm, and 71.1 cm. These preliminary results show that measurements taken in the FBBF when corrected for the decay of the californium source are reproducible to within the errors of the measurements. Further experiments, using other materials that will yield higher counting rates and hence better statistics, are planned.

Figure C.14 shows a radial traverse of manganese activity generated in Sector A. Shown as a solid line is the calculated manganese activity from the 2DB code. The calculations predict the general shape of the experimental curve but fail to predict the actual activities. The fact that the cross sections used in the calculations were self-shielded for a modified Clinch River Breeder Reactor at 1000°K while the FBBF operates at room temperature is considered to be a primary contributor to the discrepancies found. Additional comparisons between calculated and experimental activity distributions are planned when the improved cross section set is available (see Sec. B.3).

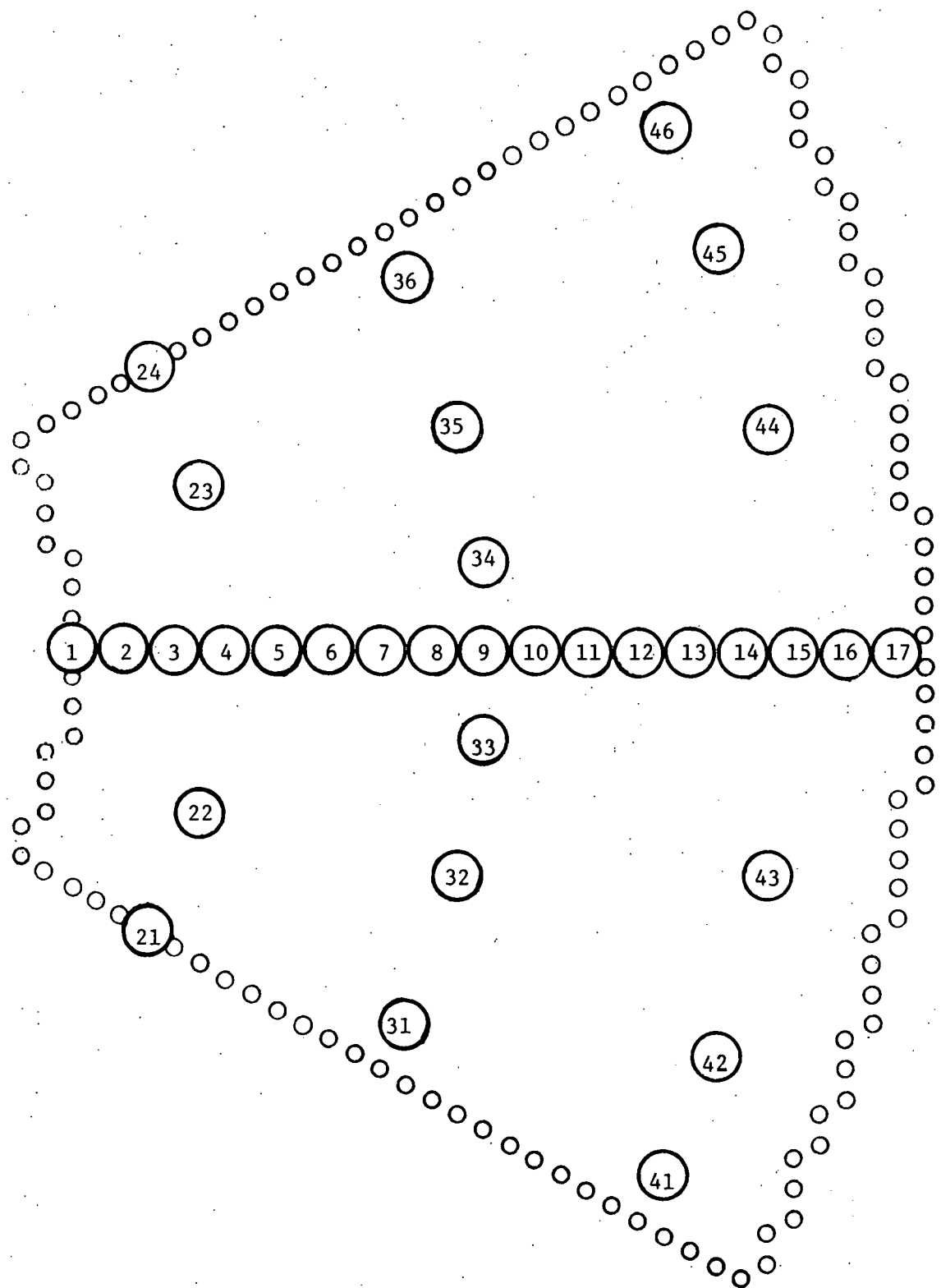


Figure C.4: Radial and Azimuthal Positions.

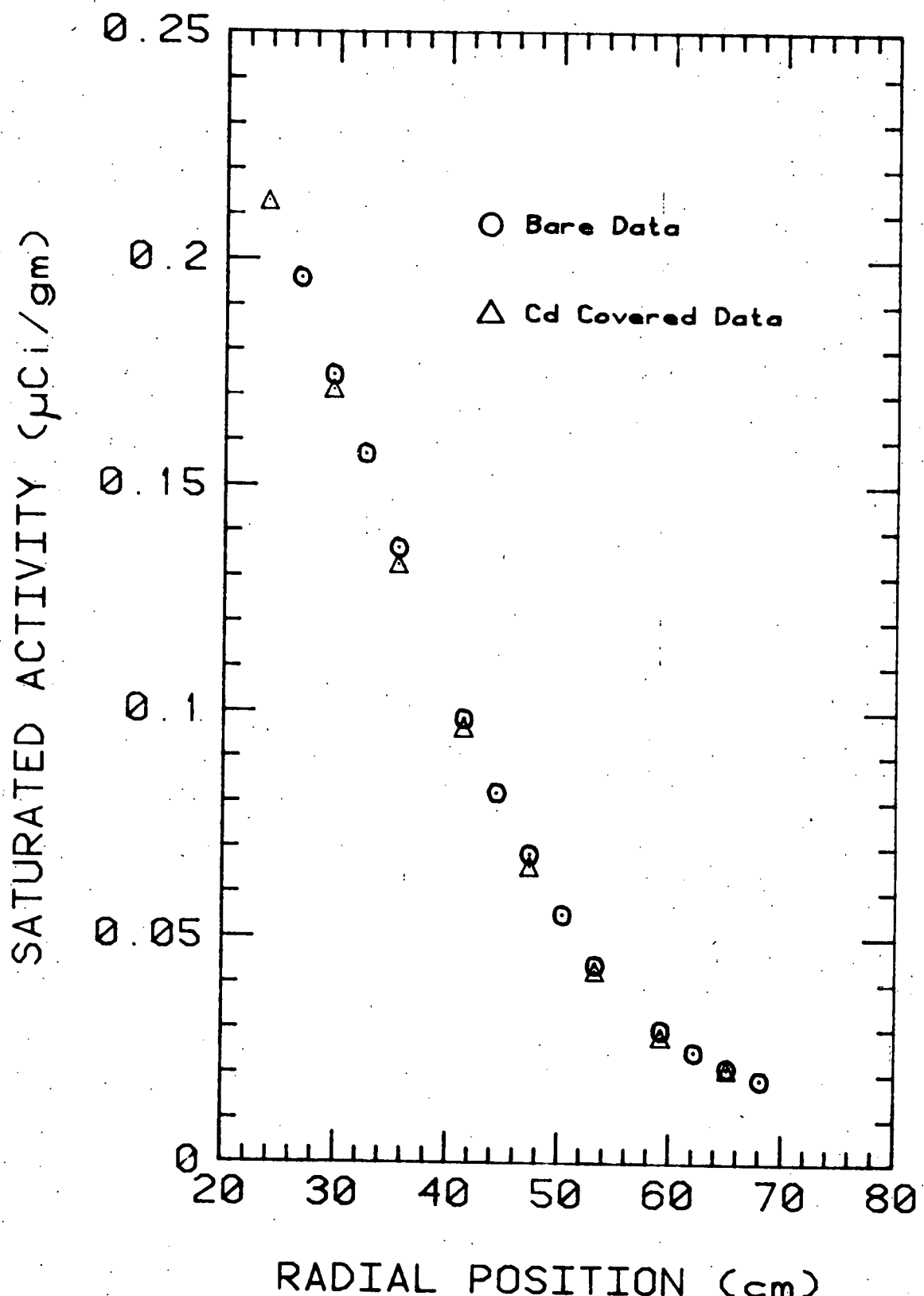


Figure C.5: Radial traverse of gold saturated activities both bare and cadmium covered. The errors in the dots are less than the height of the symbols used.

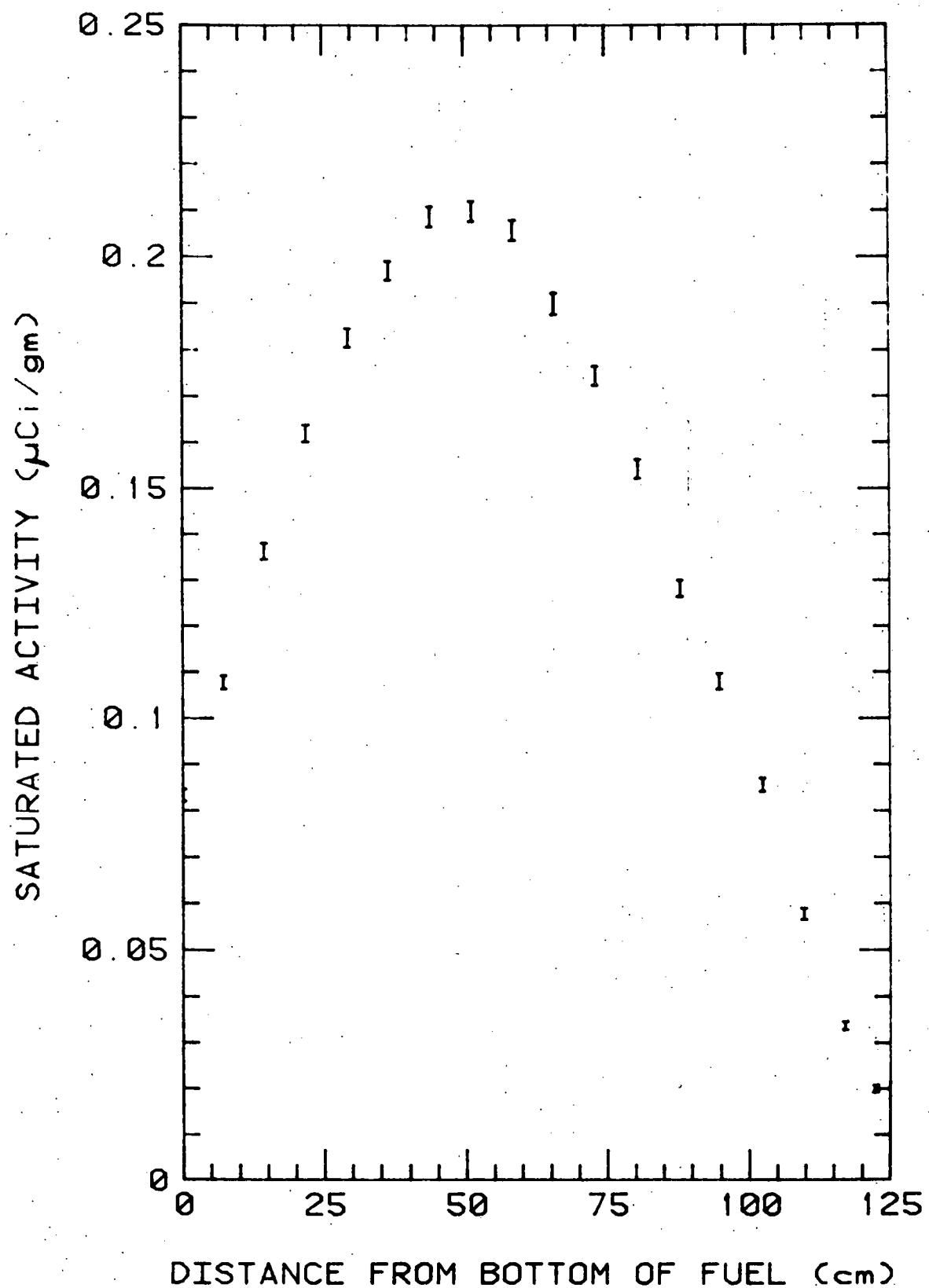


Figure C.6: Axial traverse of bare gold activity at position A-1.

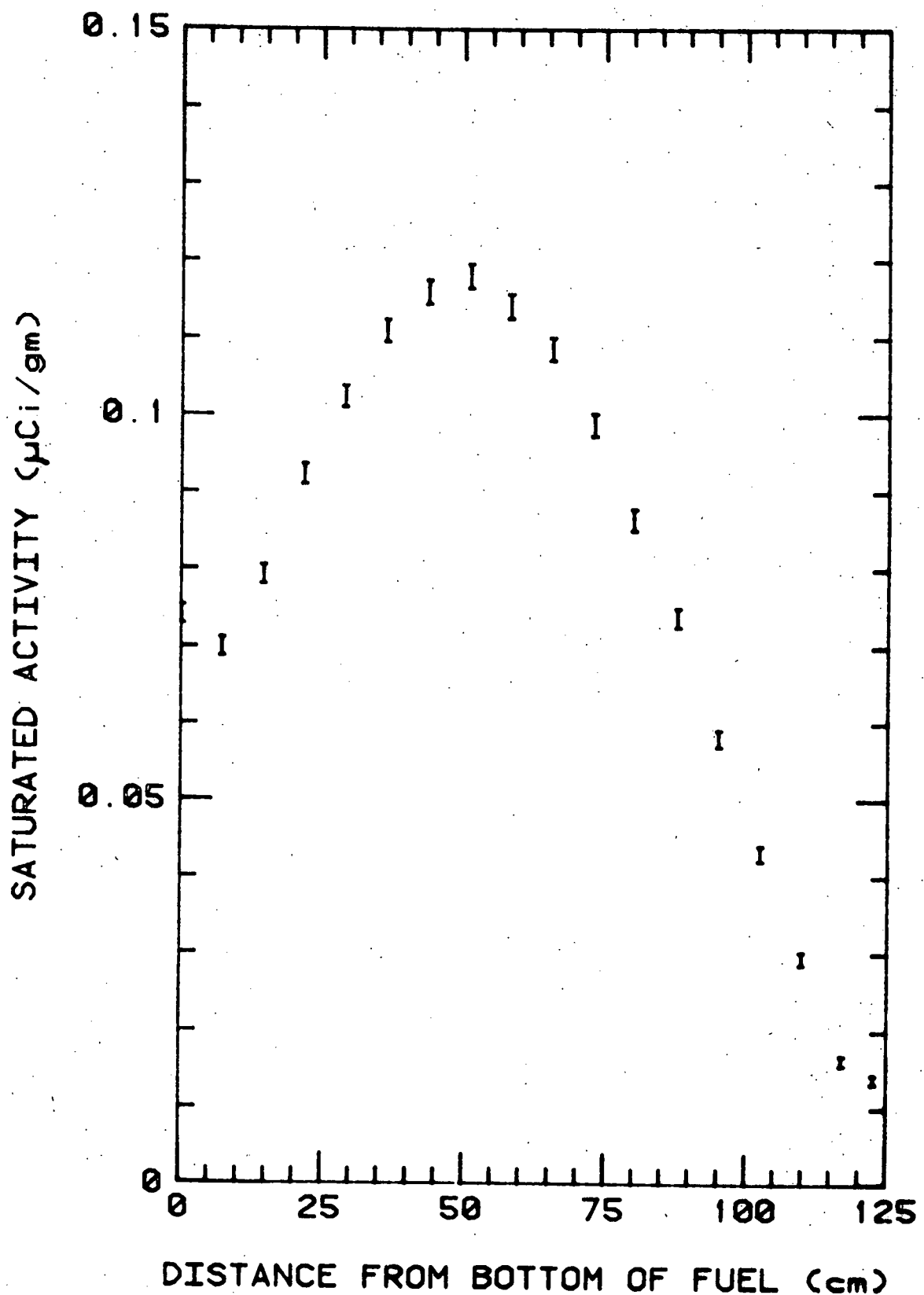


Figure C.7: Axial traverse of bare gold activity at position A-6.

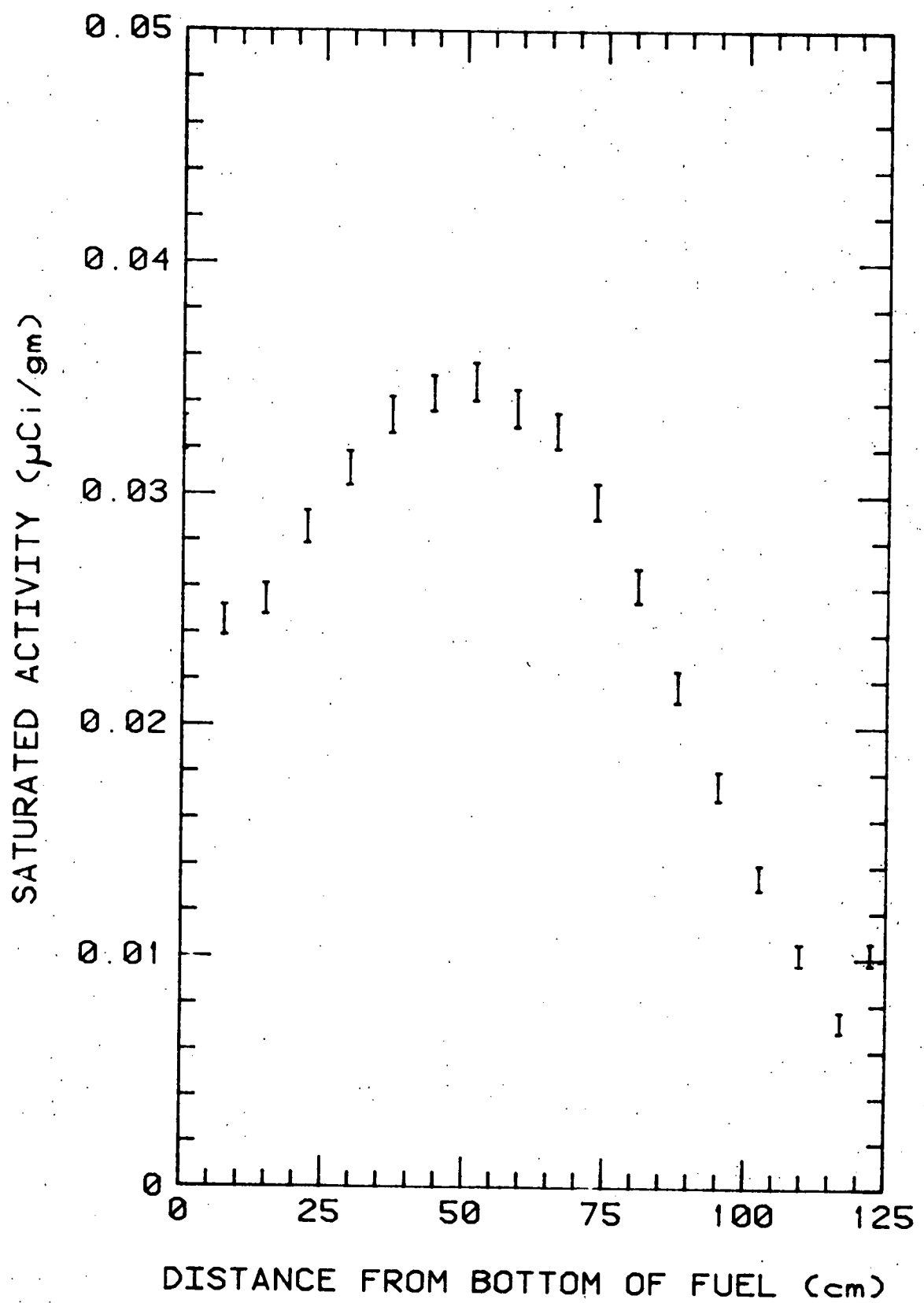


Figure C.8: Axial traverse of bare gold activity at position A-12.

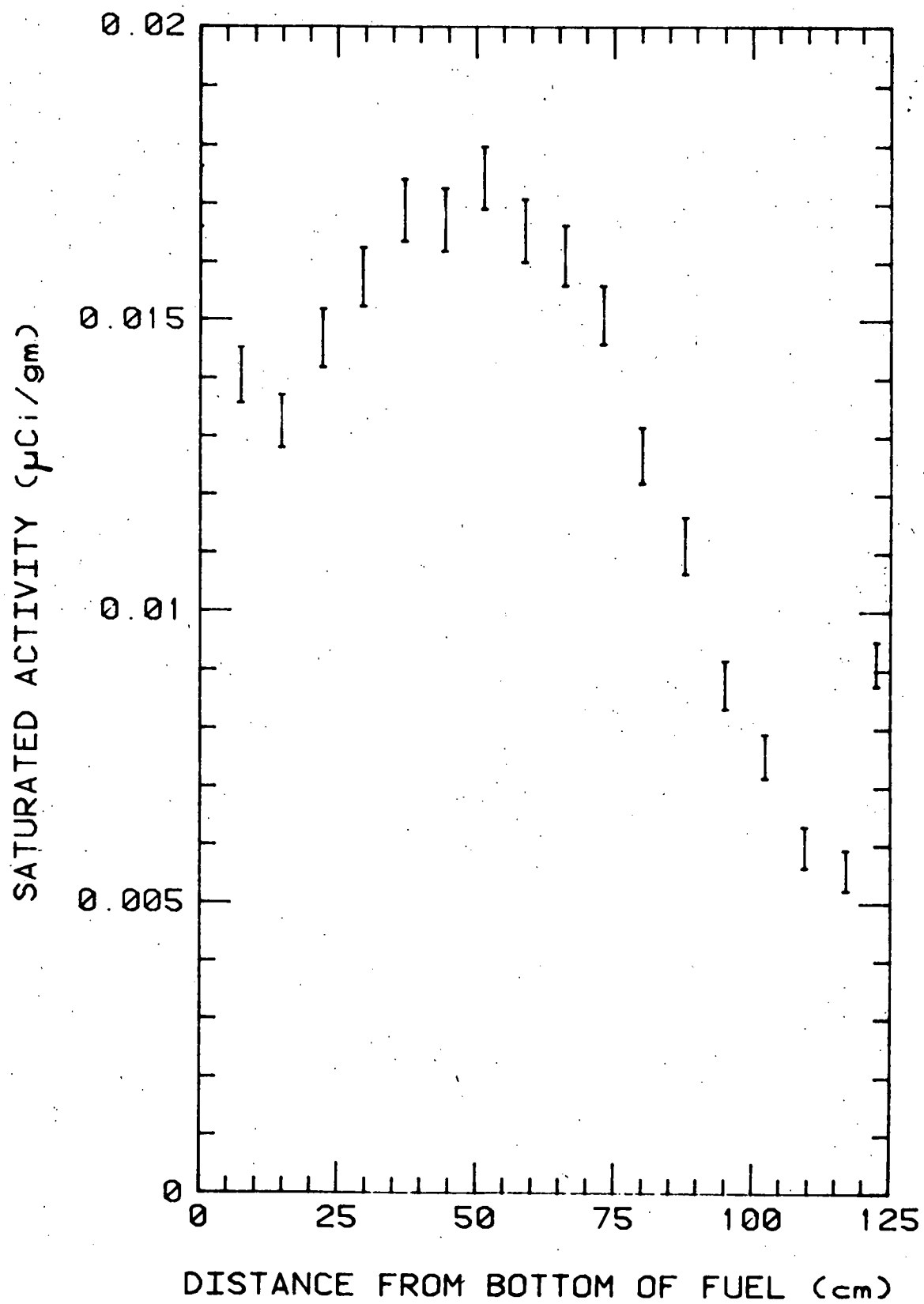


Figure C.9: Axial traverse of bare gold activity at position A-17.

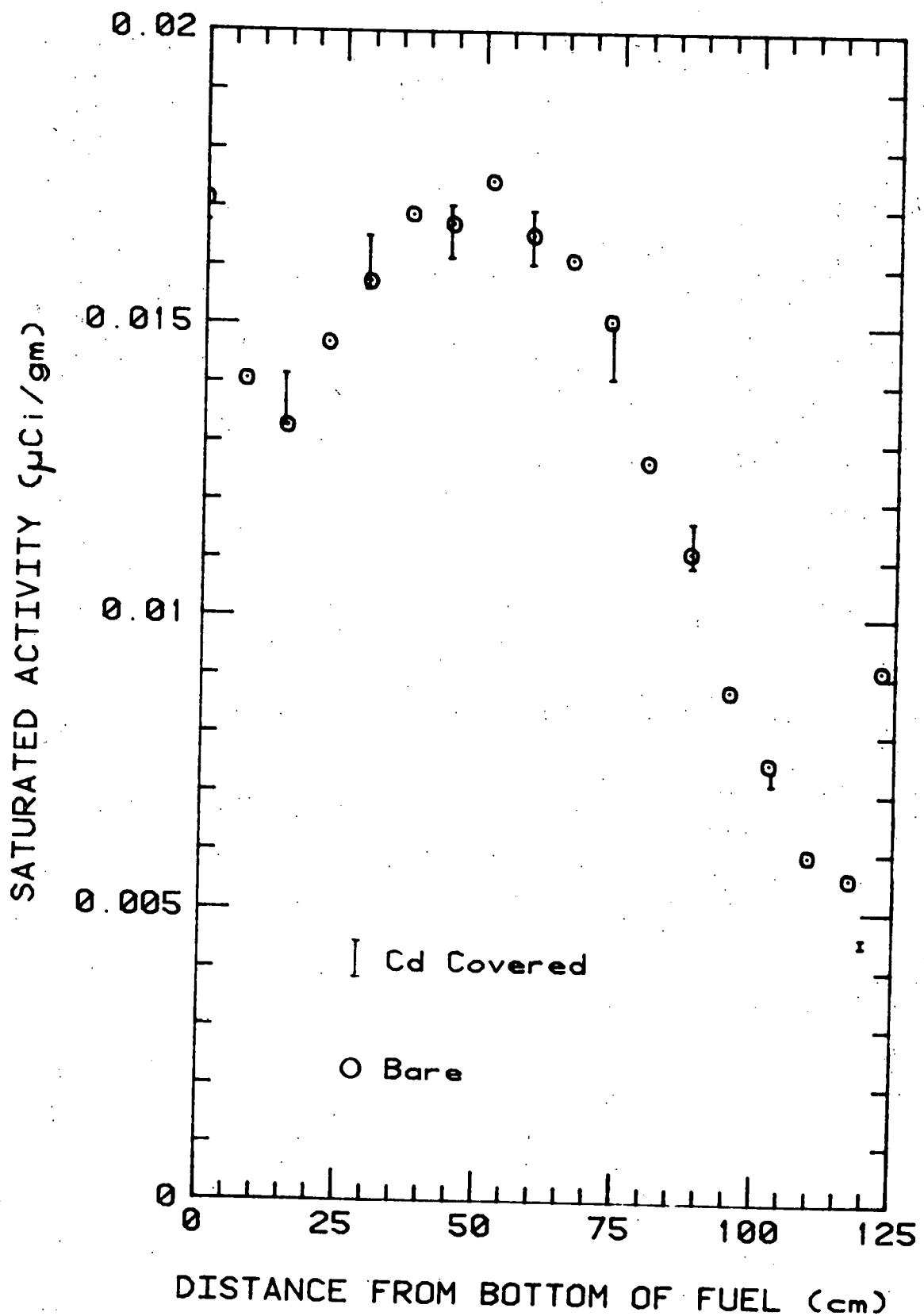


Figure C.10: Axial traverse of gold activity both bare (circles) and cadmium covered (error bars).

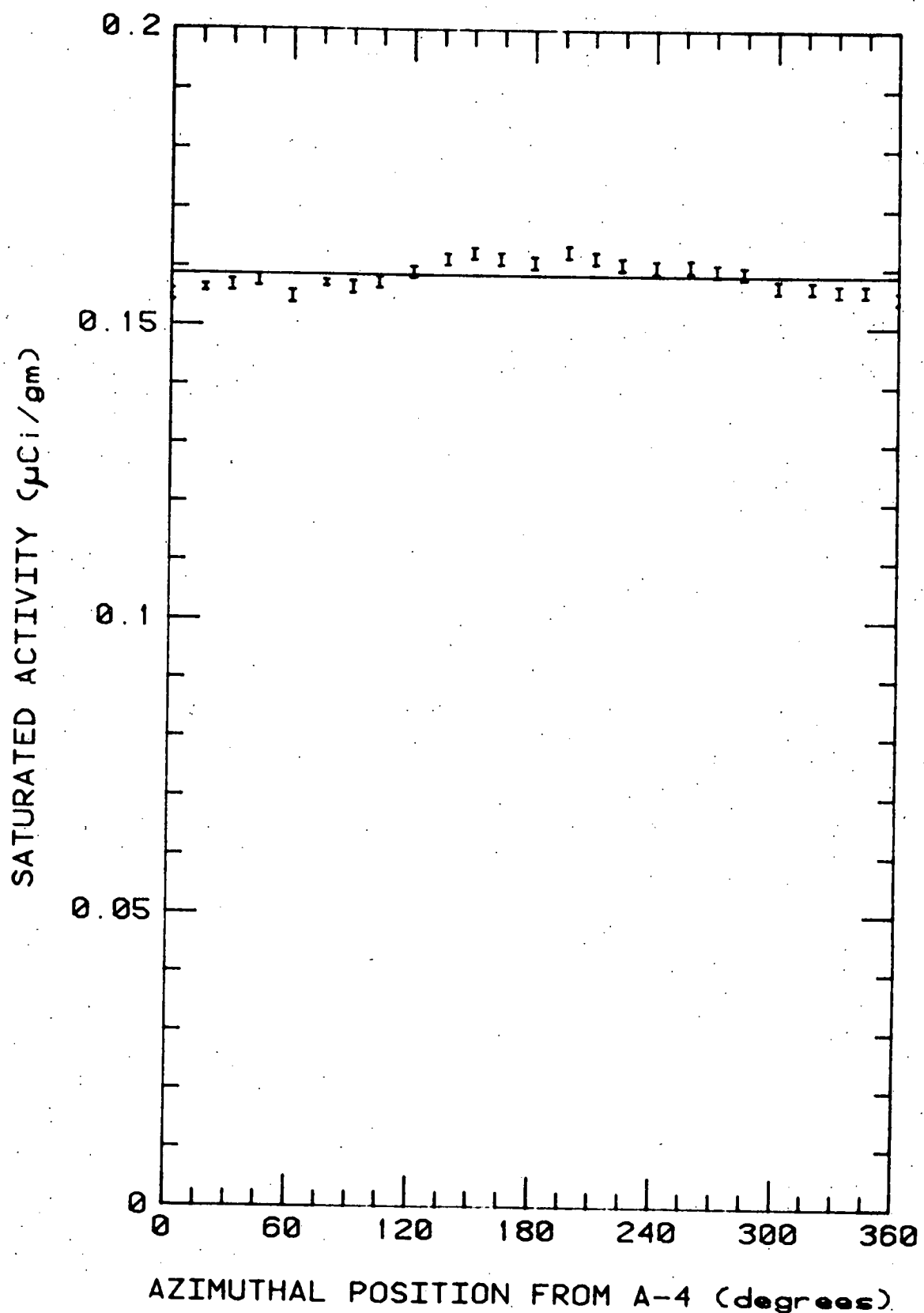


Figure C.11: Azimuthal traverse of bare gold activity at radius 32.5 cm. The solid line is the average value at all measurements.

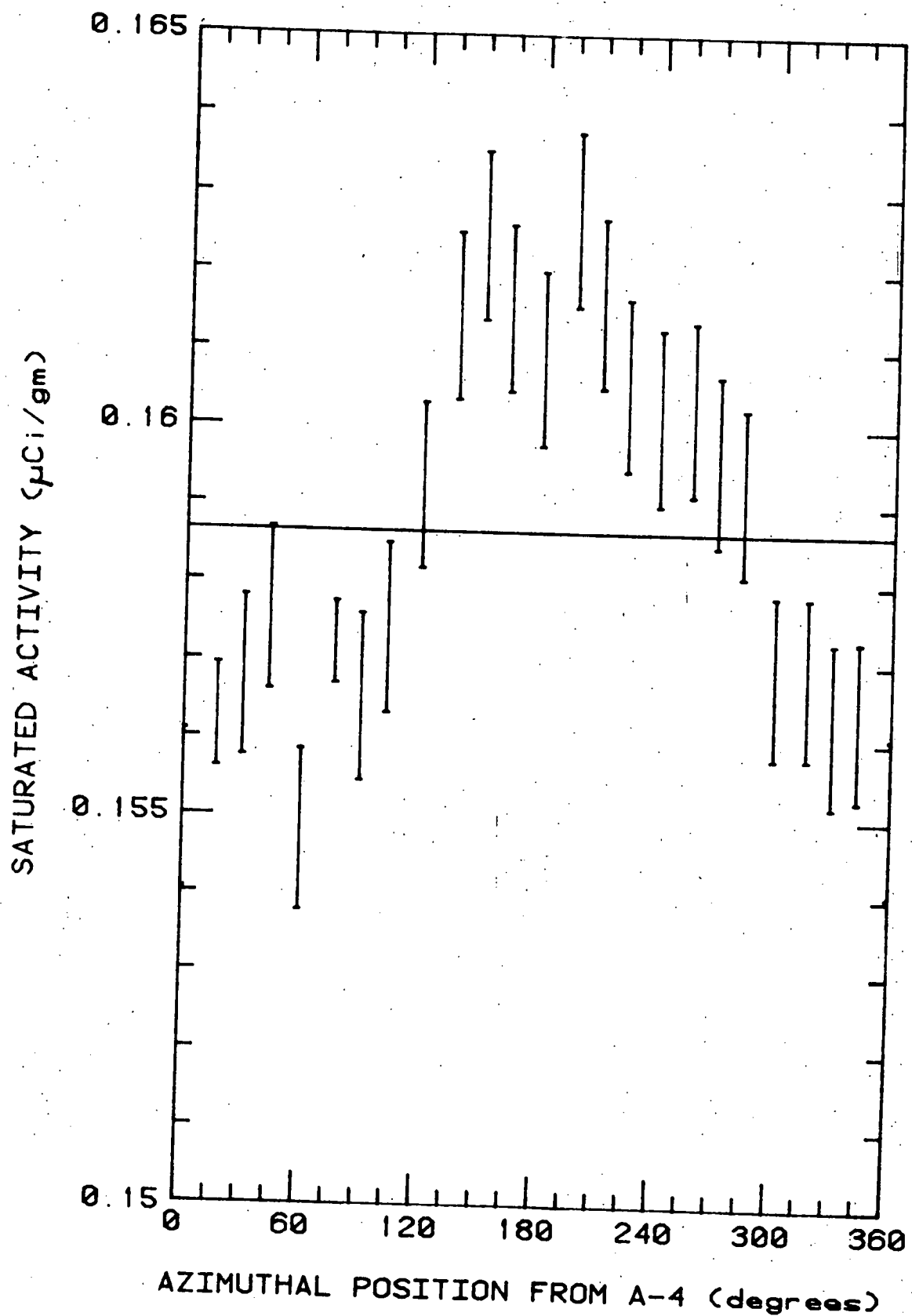


Figure C.12: Azimuthal traverse of bare gold activity at radius 32.5 cm. (zero suppressed). The solid line is the average of all measurements.

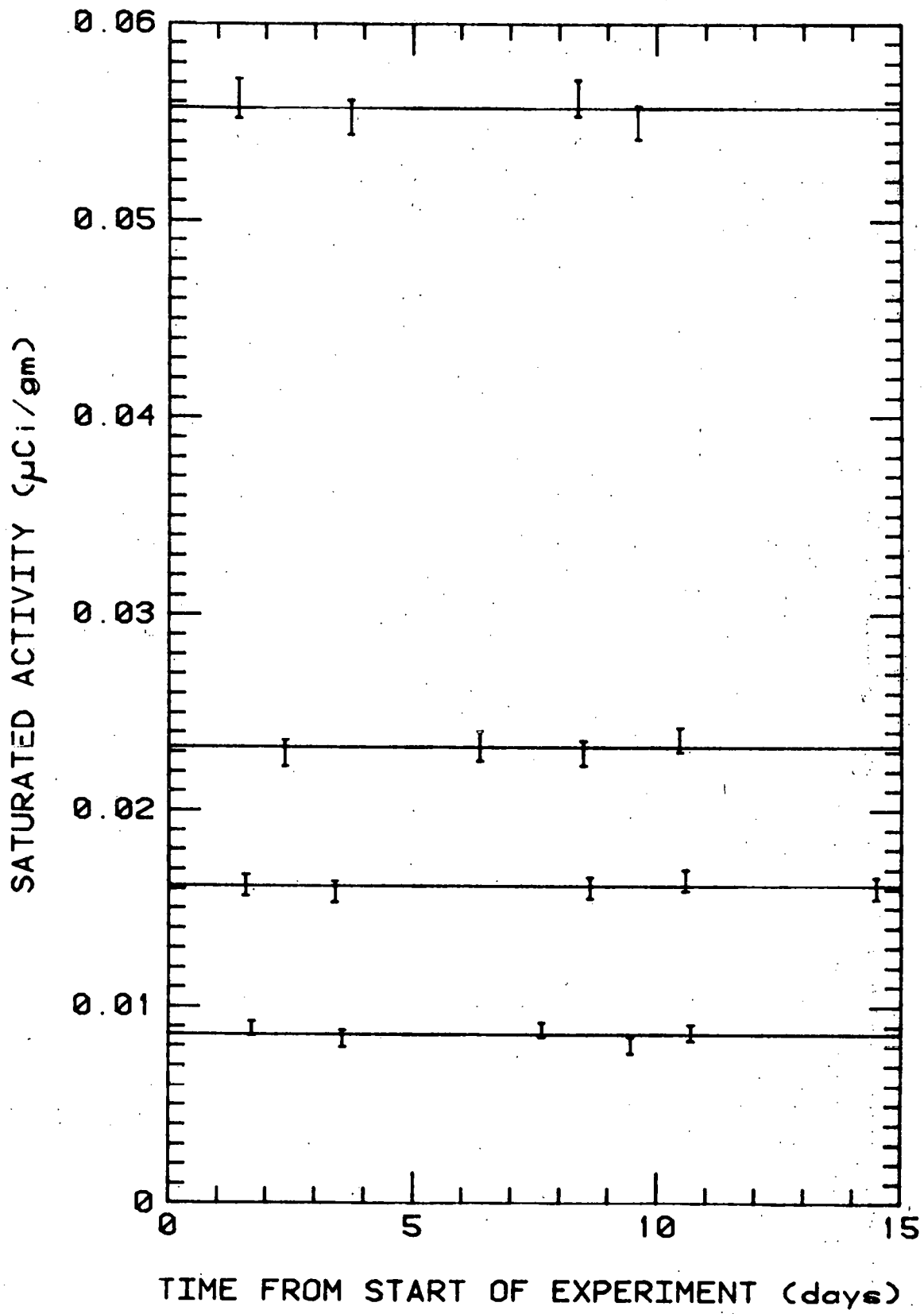


Figure C.13: Reproducibility test of the FBBF using manganese foils. The solid lines indicate the average activity at each position. The measurements were taken radially at 23.7 cm, 50.3 cm, 56.3 cm, and 71.1 cm (top to bottom) in positions 1, 10, 12, and 17 of Sector A.

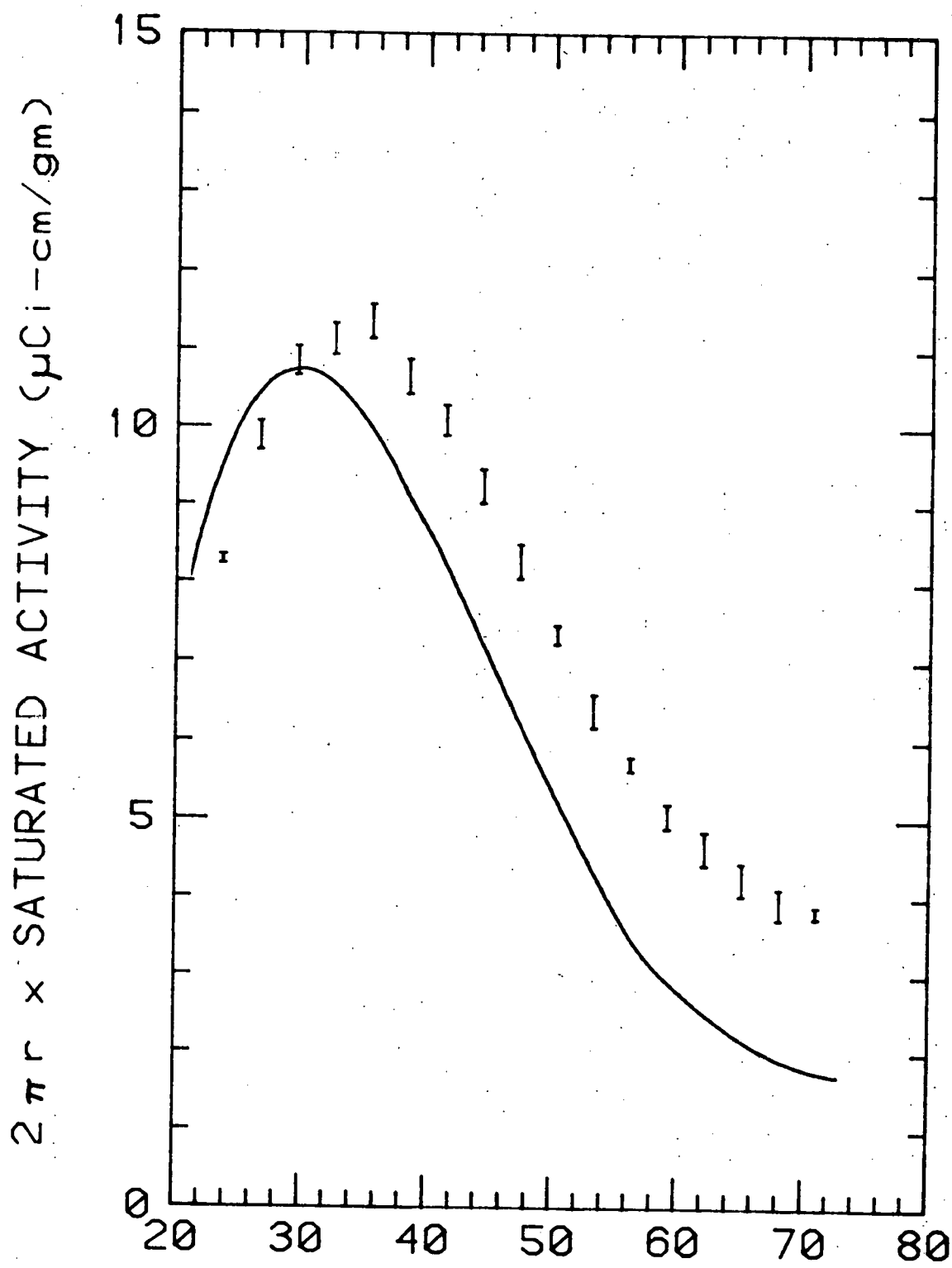


Figure C.14: Radial traverse of saturated manganese activity. Error bars indicate experimental results and the solid line shows the calculated results from the two dimensional diffusion code 2DB.

TABLE C.3

Position	Radial Location cm	Azimuthal Location off center (degrees)
1	23.69	0
2	26.65	0
3	29.61	0
4	32.57	0
5	35.53	0
6	38.49	0
7	41.45	0
8	44.41	0
9	47.37	0
10	50.33	0
11	53.29	0
12	56.26	0
13	59.22	0
14	62.18	0
15	65.14	0
16	68.10	0
17	71.06	0
21	32.48	30
22	32.48	16.83
23	32.48	16.83
24	32.48	30
31	47.96	26.46
32	47.65	15.61
33	47.65	6.18
34	47.65	6.18
35	47.65	15.61
36	47.96	26.46
41	65.03	27.39
42	64.94	20.82
43	64.94	11.39
44	64.94	20.82
45	64.94	27.39
46	65.03	

REFERENCES

1. R.H. Johnson and J.H. Paczolt, "Experience with the DLC-37/EPR Cross Section Library for Preliminary Gamma-Ray Heating Analysis of the Purdue University Fast Breeder Blanket Facility," Proc. RSIC Seminar-Workshop on Multigroup Cross Sections, Oak Ridge, Tennessee, March 14-16, 1978.
2. K.O. Ott, F.M. Clikeman, P.J. Fulford, R.C. Borg, R.H. Johnson and O.H. Gilar, "The Purdue University Fast Breeder Blanket Facility," Proc. ANS Topical Meeting on Advances in Reactor Physics, p. 505, Gatlinburg, Tennessee, April 9-12, 1978, CONF-780401 (1978).
3. FBBF Quarterly Progress Report for the period Janulary 1, 1976 - August 30, 1976, Purdue University, PNE-76-115 COO-2826-1 (1976)
4. FBBF Quarterly Progress Report for the period April 1, 1977 - June 30, 1977, Purdue University, PNE-77-119, COO-2826-4 (1977).
5. D.J. Malloy, "The HAMMER System at Purdue University," PNE-76-106, October, 1975.
6. FBBF Quarterly Progress Report for the period January 1, 1978 - March 31, 1978, Purdue University, PNE-78-128, COO-2826-8 (1978).
7. R.W. Hardie and W.W. Little, Jr., "1DX, A One-Dimensional Diffusion Code for Generating Effective Nuclear Cross Sections," Battelle Pacific Northwest Laboratories, BNWL-954 (1969).
8. W.W. Little, Jr. and R.W. Hardie, "2DB, A Two-Dimensional Diffusion Burnup Code for Fast Reactor Analysis," Battelle Pacific Northwest Laboratories, BNWL-460 (1968).
9. R.B. Kidman and R.E. MacFarlane, "LIB-IV, A Library of Group Constants for Nuclear Reactor Calculations," Los Alamos Scientific Laboratory, LA-6260-MS (1976).
10. FBBF Quarterly Progress Report for the period January 1, 1978 - March 31, 1978, Purdue University, PNE-78-128, COO-2826-8 (1978).
11. R.G. Soltesz and R.K. Disney, "Nuclear Rocket Shielding Methods, Modification, Updating, and Input Data Preparation, Volume 4 -- One-Dimensional, Discrete Ordinates Transport Technique," Westinghouse Astronuclear Laboratory, WANL-PR-(LL)-034, (1970).
12. D.J. Malloy, L.B. Luck and G.L. Terpstra, "LAZARUS, A One-Dimensional Diffusion Theory Package for Fast Reactor Calculations," Purdue University, PNE-75-112 (1976).

13. K.O. Ott, K.R. Boldt and F.M. Clikeman, "Review of Nuclear Physics Uncertainties in Fast Reactor Blankets," Purdue University, PNE-75-103. K.R. Boldt, M.S. Thesis, Purdue University, (1975).
14. E.F. Bennet, T.J. Yule, "Techniques and Analysis of Fast Neutron Spectroscopy Proton-Recoil Proportional Counters," ANL-7763, (August 1971).
15. W. Binde and J.R. Cameron, "Dosimetric Properties of $\text{CaF}_2:\text{Dy}$," University of Wisconsin, COO-1105-146 (1968).
16. G.G. Simons and T.S. Huntsman, "Precision of ^7LiF Thermoluminescent Dosimeters Using Sensitivity Selection," Argonne National Laboratory, ZPR-TM-200 (1975).
17. J.E. Bigelow, Oak Ridge National Laboratory, Private Communication (1977).
18. V. Spiegel, "The Effective Half Life of Californium-252," Nucl. Sci. Eng. 53, 326 (1974).
19. C.L. Lederer, J.M. Hollander and I. Perlman, Table of Isotopes, Sixth Edition, John Wiley and Sons (1967).
20. R.H. Johnson and P.J. McDaniel, "Dose Rates Outside Concrete Shield," FBBF Quarterly Progress Report for Period January 1, 1976 - August 30, 1976, pp. 36-45, COO-2826-1.
21. R.C. Borg and D.J. Malloy, "Neutron Flux Calculations for Initial FBBF Loading," FBBF Quarterly Progress Report for Period January 1, 1976 - August 30, 1976, pp. 16-34, COO-2826-1.